A zebrafish embryo screen utilizing gastrulation for identification of anti-metastasis drugs

Joji Nakayama[1,2,3,§], Hideki Makinoshima[1,4] , and Zhiyuan Gong[3]

[1]Tsuruoka Metabolomics Laboratory, National Cancer Center, Tsuruoka, Japan

[2]Shonai Regional Industry Promotion Center, Tsuruoka, Japan.

[3]Department of Biological Science, National University of Singapore, Singapore

[4]Division of Translational Research, Exploratory Oncology Research, and Clinical Trial Center, National Cancer Center, Kashiwa, Japan.

[§]Corresponding author:

Joji Nakayama

Tsuruoka Metabolomics Laboratory, National Cancer Center, Mizukami 246-2, Kakuganji, Tsuruoka, Yamagata, Japan 975-0052.

E-mail: zmetastasis@gmail.com

ORCID: 0000-0003-1077-140X

Tel: +81-235-64-0980

Keywords: Metastasis, gastrulation, EMT, Phenotyping screening, zebrafish

Total words excluding references and figure legends: 2354

Number of figures: 4

Number of tables: 1

Abstract

Few models exist that allow for rapid and effective screening of anti-metastasis drugs. Here, we present a phenotype-based chemical screen utilizing gastrulation of zebrafish embryos for identification of anti-metastasis drugs. Based on the evidence that metastasis proceeds through utilizing the molecular mechanisms of gastrulation, we hypothesize that chemicals which interrupt zebrafish gastrulation might suppress metastasis of cancer cells. Thus, we developed a drug screening protocol which uses epiboly, the first morphogenetic movement in gastrulation, as a marker. The screen only needs zebrafish embryos and enables hundreds of chemicals to be tested in five hours through observing epiboly progression of a test chemical-treated embryos. In the screen, embryos at the two-cell stage are firstly corrected and then developed to the sphere stage. The embryos are treated with a test chemical and incubated in the presence of the chemical until vehicle-treated embryos develop to 90% epiboly stage. Finally, positive 'hit' chemicals that interrupt epiboly progression are selected through comparing epiboly progression of the chemical-treated embryos with that of vehicle-treated embryos under a stereoscopic microscope. Previous study subjected 1,280 FDA-approved drugs to the screen and identified Adrenosterone and Pizotifen as epiboly-interrupting drugs. These drugs were validated to suppress metastasis of breast cancer cells in mice models of metastasis. Furthermore, 11β–Hydroxysteroid Dehydrogenase 1 (HSD11β1) and serotonin receptor 2C (HTR2C), which are primary target of Adrenosterone and Pizotifen respectively, promotes metastasis through induction of epithelial-mesenchymal transition (EMT). That indicates the screen could be diverted to a chemical genetic screening platform for identification of metastasis-promoting genes.

Introduction

Cancer research using zebrafish as a model has attracted attention because this model offers many unique advantages that are not readily provided by other animal models. Futhermore, the zebrafish system has been increasingly recognized as a platform for chemical screening because it provides the advantage of high-throughput screening in an in vivo vertebrate setting with physiologic relevance to humans [1-5].

Metastasis is responsible for approximately 90% of cancer-associated mortality. It proceeds through multiple steps: invasion, intravasation, survival in the circulatory system, extravasation, colonization, and metastatic tumor formation in secondary organs with angiogenesis [6-8]. Dissemination of cancer cells is an initial step of metastasis and its molecular mechanism involves local breakdown of basement membrane, loss of cell polarity, and induction of EMT [9,10]. These cellular and biological phenomena are also observed during vertebrate gastrulation in that evolutionarily conserved morphogenetic movements of epiboly, internalization, convergence, and extension cooperate to generate germ layers and sculpt the body plan [11]. In zebrafish, the first morphogenetic movement, epiboly, is initiated at approximately four hours post-fertilization (hpf) to move cells from the animal pole to eventually engulf the entire yolk cell by 10 hpf. These movements are governed by the molecular mechanisms that are induced by temporally and spatially regulated gene expression, and these mechanisms and changes in gene expression are partially observed in metastatic progression [12].

Development of the protocol

Metastasis proceeds through utilizing the molecular mechanisms of gastrulation. At least fifty common genes were shown to be involved in both gastrulation and metastasis progression (Table 1) [13-17]. The fifty genes are expressed in Xenopus or zebrafish embryos, and genetic inhibition of each of the fifty genes in these embryos interferes with gastrulation progression. Conversely, the same fifty genes are ectopically expressed in metastatic cancer cells and confer metastatic

properties on cancer cells, and genetic inhibition of each of the fifty genes suppresses metastasis progression. These evidences led us to hypothesize that chemicals which interfere with zebrafish gastrulation might suppress metastasis progression of cancer cells. Based on the hypothesis, we developed a drug screening protocol which uses epiboly, the first morphogenetic movement in gastrulation, as a marker. This screen measures the suppressor effect of each of test chemicals through observing epiboly progression of the chemical-treated embryos (Fig. 1 and Fig. 2).

Applications of the method

This screen enables hundreds of chemicals to be tested in five hours. Our study subjected 1280 FDA-approved drugs to this screen and identified Adrenosterone and Pizotifen as epiboly-interfering drugs. These drugs were further validated to suppress metastasis of breast cancer cells in mouse models of metastasis (Fig. 3) [18,19]. This screen can also measure suppressor effect of crude drugs. We subjected 120 herbal medicines to this screen and identified cinnamon bark extract as an epiboly-interfering drug. Cinnamon bark extract was validated to suppress metastatic dissemination of breast cancer cells in zebrafish xenograft model [20]. Moreover, this screen can be diverted to a chemical genetic screening platform for identification of metastasis-promoting genes. HSD11β1 and HTR2C, which are respectively primary targets of Adrenosterone and Pizotifen, induce EMT and promote metastasis of breast cancer cells (Fig. 4) [18,19].

Comparison with other methods

Current mouse models of metastasis are too expensive and time-consuming to use for rapid and high-throughput screening [21,22]. Also in vitro model of metastatic dissemination such as a Boyden chamber assay can test a limited number of chemicals in one assay and needs huge time and effort in analyzing the results [23]. In contrast, our screen only needs zebrafish embryos and enables hundreds of chemicals to be tested in five hours through observing epiboly progression of a test

chemical-treated embryos. Furthermore, out of the 78 chemicals which interrupt epiboly progression of zebrafish embryos, 20 of the chemicals were validated to suppress cell motility and invasion of highly metastatic human cancer cells without affecting cell viability in a Boyden chamber assay. Among the 20 chemicals, Adrenosterone and Pizotifen were validated to suppress metastasis of breast cancer cells in mice models of metastasis [18,19]. A disadvantage of this screen is that zebrafish have orthologues to 86% of 1318 human drug targets [27]. Therefore, 75% of the chemicals which interrupt epiboly progression of zebrafish embryos, fail to suppress cell motility and invasion of highly metastatic human cancer cells in a Boyden chamber assay [19].

Experimental design

This screen measures suppressor effect of each of chemicals based on epiboly progression of zebrafish embryos. Niclosamid or DMSO is used as positive or negative control, respectively. Epiboly progression of each of chemical treated embryos is compared with that of DMSO-treated embryos. Firstly, embryos at the two-cell stage are firstly corrected and then developed to the sphere stage. The embryos are treated with a test chemical and incubated in the presence of the chemical until vehicle-treated embryos develop to 90% epiboly stage. Finally, positive 'hit' chemicals that interrupt epiboly progression are selected through comparing epiboly progression of the chemical-treated embryos with that of vehicle-treated embryos under a stereoscopic microscope [19].

Limitations

There is a limitation in delivering chemicals to zebrafish embryos. Zebrafish embryos are surrounded by the acellular chorion, which is known to be about 1.5–2.5 μm thick and to consist of three layers pierced by pore canals. The pore allows passage of water, ions, and chemicals. A study reported molecules which are larger than 3-4 KDa fail to pass through the chorion.

Therefore, this screen may not be able to measure suppressor effect of the molecules which are larger than 3-4 KDa [28].

Materials

REAGENTS

- Wild-type zebrafish strain
- E3 medium (5.0 mM NaCl, 0.17 mM KCl, 0.33 mM $MgSO_4$)
- FDA, EMA, and other agencies-approved chemical libraries were purchased from Prestwick Chemical (Illkirch, France).
- Niclosamid
- DMSO

EQUIPMENT

- 24-well flat bottom plastic plates (Corning)
- Stereomicroscope (MZ75, Leica)
- Incubator (Thermo)

Procedure

Zebrafish mating setup (Day 0) _Timing 10 mins

1. On the night before collecting embryos, arrange male and female zebrafish in pairs separated by a divider

   CRITICAL STEP

   Young adult zebrafish should be used for the crossing. Qualities of zebrafish embryos affect screening efficiency.

Embryo collection, and distribution (Day 1) _Timing 10-30 min

2. Remove the divider to allow the fish to spawn.
3. To obtain zebrafish embryos of the same development stage, zebrafish were crossed for 10 mins. If more than twenty chemicals were tested, the crossing were conducted three times at three different time points (Group A_8:30, Group B_9:00 and Group C_9:30AM).
4. After 10 mins, set back divider to prevent zebrafish from spawning.

   CRITICAL STEP

   This screen measures suppressor effect of each chemical on progression of epiboly in live zebrafish embryos. Therefore, epiboly proceeds during measuring the effect under a stereoscopic microscope. If more than 20 chemicals are tested, screening should be divided into more than two sessions and each of the sessions start at different time point. For example, if 60 chemicals are screened, zebrafish should be crossed at three different time points over 30 mins apart. To do that, 30 mins for measuring the effects would be ensured.
5. Collect the embryos and remove dead embryos
6. Incubate the embryos at 27 ˚C for twenty mins
7. Collect embryos at the two-cell stage under stereoscopic microscope.
8. Array approximately twenty embryos into each well of a 24-well plate
9. Remove E3 medium from each well including the embryos by using a pipet
10. Add 900 µl of E3 medium to the well.

Embryo development to the sphere stage_Timing 4 hours

11. Incubate the embryos at 27 ˚C until the embryos develop to the sphere stage

    CRITICAL STEP

    The temperature of E3 medium affects the rate of development of zebrafish embryos. Higher temperature accelerates the rate; conversely, lower temperature slows the rate [29].

176 Therefore, non-uniform temperature between E3 medium of each well of 24-well plate
177 containing zebrafish embryos would cause false positive.
178
179 **Addition of chemicals_Timing 30 mins**
180 12. At 30 mins before adding test chemicals to embryos, prepare 10-fold concentration of
181 each of the chemicals in E3 medium
182 13. Add 100 µl of 10-fold concentration of the medium to 900 µl of E3 medium containing
183 zebrafish embryos when the embryos develop to the sphere stage.
184 14. For example, for 60 test chemicals to be screened, they are divided into three groups.
185 a. First 20 test chemicals plus Niclosamid as positive control, and DMSO as negative
186 control are added into group A when embryos from group A develop to sphere stage.
187 b. Second 20 test chemicals plus Niclosamid, and DMSO were added into group B when
188 embryos from group B develop to sphere stage.
189 c. Last 20 test chemicals plus Niclosamid, and DMSO were added into group C when
190 embryos from group C develop to sphere stage
191
192 **Development of DMSO-treated embryos to 90% epiboly stage_Timing 5 hours**
193 15. After the addition of test chemicals, the embryos are incubated at 27 ˚C for approximately
194 five hours.
195 CRITICAL STEP
196 The temperature of E3 medium affects the rate of development of zebrafish embryos. Non-
197 uniform temperature between E3 medium of each well of 24-well plate containing zebrafish
198 embryos would cause false positive.
199
200 **Measuring the inhibition effects of each of chemicals_Timing 30 mins**

16. Comparing epiboly progression of each of chemicals-treated embryos from group A with that of DMSO-treated embryos from group A under the stereoscopic microscope when DMSO-treated embryos from group A develop to 90% epiboly stage.
17. After approximately 30 min from observing embryos in group A, measuring the inhibition effects of each of chemicals on epiboly progression of embryos in group B and when DMSO-treated embryos from group B develop to 90% epiboly stage.
18. After approximately 30 mis from observing embryos in group B, measuring the inhibition effects of each of chemicals on epiboly progression of embryos in group C and when DMSO-treated embryos in group C develop to 90% epiboly stage.

CRITICAL STEP

Epiboly proceeds during comparing epiboly progression of each of chemicals-treated embryos with that of DMSO-treated embryos under the stereoscopic microscope. Therefore, measuring the effect should be done in 30 mins.

Timing

Step 1, Zebrafish mating setup: overnight

Step 2-5, Crossing zebrafish: 10 mins

Step 6, Develop the embryos to the two-cell stage

Step 7, Collect two cell stage embryos: 20 mins

Step 8-10, Array 20 embryos into each well of 24-well plate: 30 mins

Step 11, Develop the embryos to sphere stage: 4 hours

Step 12-14, Prepare chemical drugs in E3 medium and add the medium into each well of 24-well plate: 30 mins

Step 15, Develop the embryos to 90% epiboly stage: 5 hours

Step 16-18, measuring epiboly progression: 30 mins

227 **Troubleshooting**

228 Qualities of zebrafish embryos affect screening efficiency. Low qualities of embryos show high
229 frequencies of abnormal embryos with asymmetric cell cleavage, and development of the
230 embryos arrest at early cleavage stages [30]. If a screen used low qualities of zebrafish embryos, it
231 would generate false 'hit' chemicals since suppressor effect of a test chemical is measured by
232 observing epiboly progression of the chemical-treated embryos. If the number of zebrafish
233 embryos showing morphological abnormalities correlate with final concentration of a test
234 chemical, the abnormalities may result from an effect of the test chemical on the embryos.

235

236 **Anticipated results**

237 Suppressor effects of a tested chemical on epiboly progression of zebrafish embryos are
238 significantly affected by final concentration of the chemical. Previous study subjected 1,280
239 FDA-approved drugs to the screen and showed 6% (78/1280) of the tested drugs affected epiboly
240 progression of the embryos when the embryos were treated with 10 μM. Out of the 78 epiboly-
241 interrupting drugs, 25% of the drugs succeed to suppress cell motility and invasion of highly
242 metastatic human cancer cells in a Boyden chamber assay. In contrast, epiboly progression was
243 affected more severely when the embryos were treated at 50 μM. 10.3% (132/1280) of the tested
244 drugs affected epiboly progression of the embryos, but 85 % (112/132) of the epiboly-
245 interrupting drugs failed to suppress cell motility and invasion of highly metastatic human cancer
246 cells in a Boyden chamber assay [19].

247

248 **Author contributions statements**

249 J.N. created a concept of this screen, designed research, conducted experiments, analyzed data,
250 wrote an original draft, supervised this project; H.M. and Z.G. administered this project, acquired
251 funding. All authors reviewed and edited the draft.

252

253 **ORCID for corresponding author**

254 ORCID: Joji Nakayama, 0000-0003-1077-140X

255

256 **Acknowledgments**

257 We thank Dr. Herrick (Albany Medical College) for providing pCMV-h5TH2C-VSV with us.
258 Illustrations of Fig. 1 were drawn by Ami Inoue (Kyoto University of the Arts). This study was
259 funded by grants from National Medical Research Council of Singapore (R-154000547511) and
260 Ministry of Education of Singapore (R-154000A23112 and R154000B88112) to ZG.
261 Experiments using mice were supported in part by research funds from the Yamagata prefectural
262 government and the City of Tsuruoka.

263

264 **Competing interests**

265 J.N., H.M., and Z.G. declare no conflict of interest.

266

267 **Fig. 1**

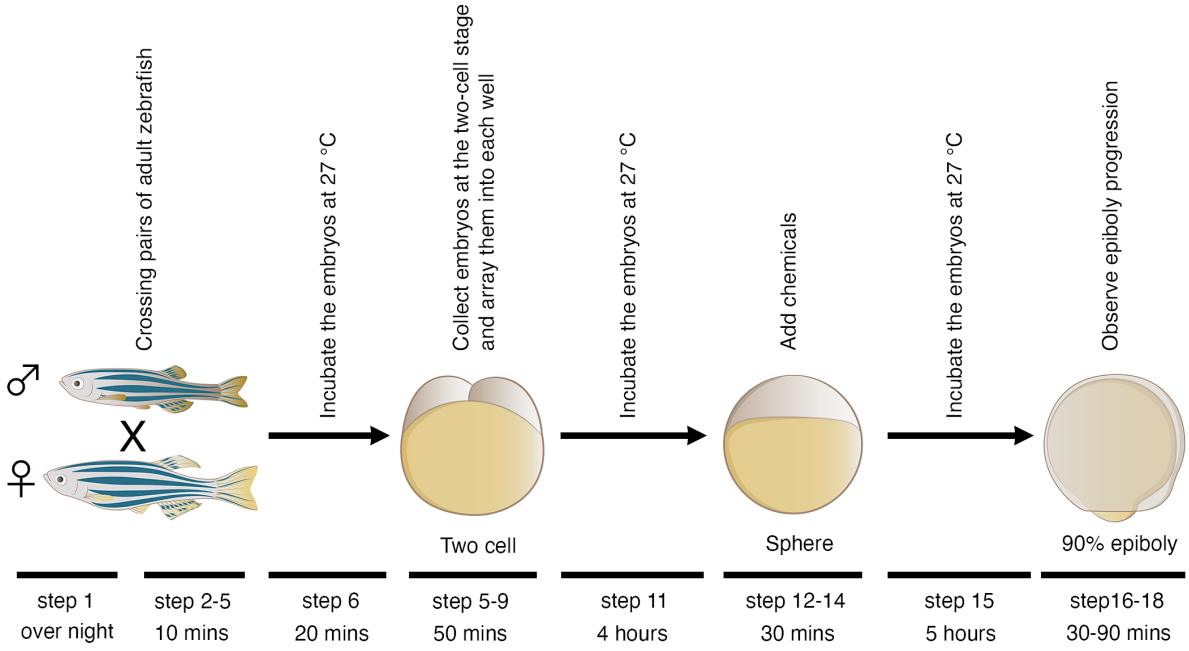

268

269 **Fig. 1_Graphic schematic of a phenotype-based chemical screen using zebrafish embryos**

270 Pairs of adult zebrafish are crossed and their embryos at the two-cell stage are collected and
271 arrayed into individual wells of 24-well plate. Chemicals are added into each well when the
272 embryos develop to the sphere stage. Epiboly progression of each of chemicals-treated embryos
273 are compared with that of DMSO-treated embryos under a stereoscopic microscope when
274 DMSO-treated embryos develop to 90% epiboly stage.

275

276 **Fig. 2**

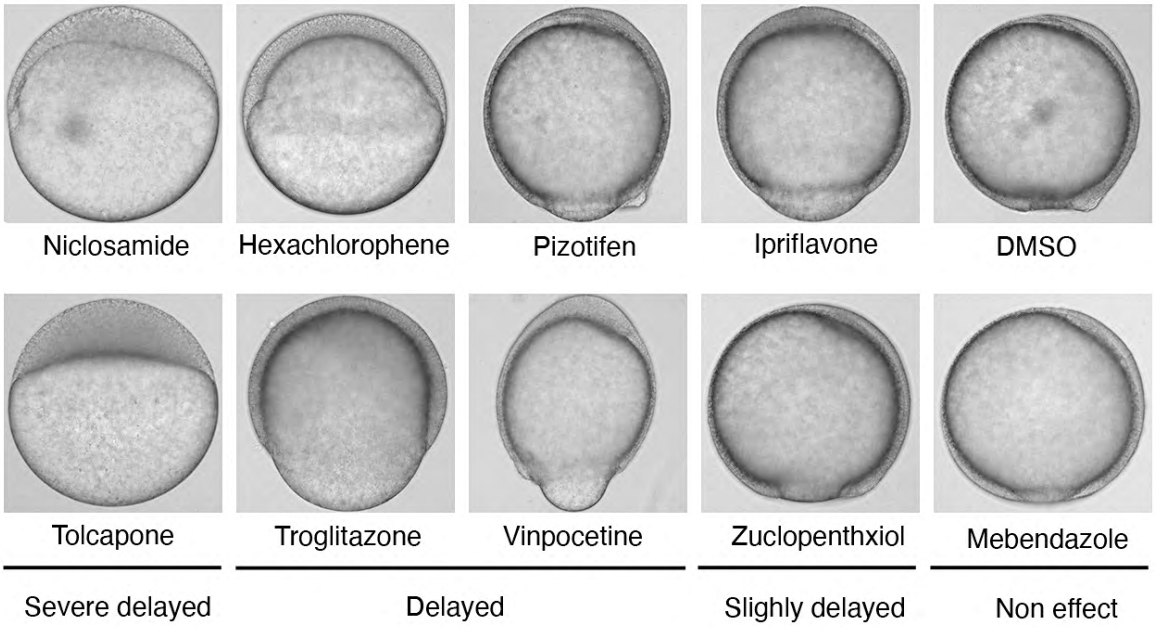

277

278 **Fig. 2_Representative samples of the embryos that were treated with indicated chemicals.**

279 Indicated chemicals were added when the embryos develop to the sphere stage. Embryos were

280 treated with 10 μM. Niclosamide-treated embryos serve as positive control and DMSO-treated

281 embryos serve as negative control. Epiboly progression of each of chemicals-treated embryos are

282 compared with that of DMSO-treated embryos under a stereoscopic microscope when DMSO-

283 treated embryos develop to 90% epiboly stage.

284 **Fig. 3**

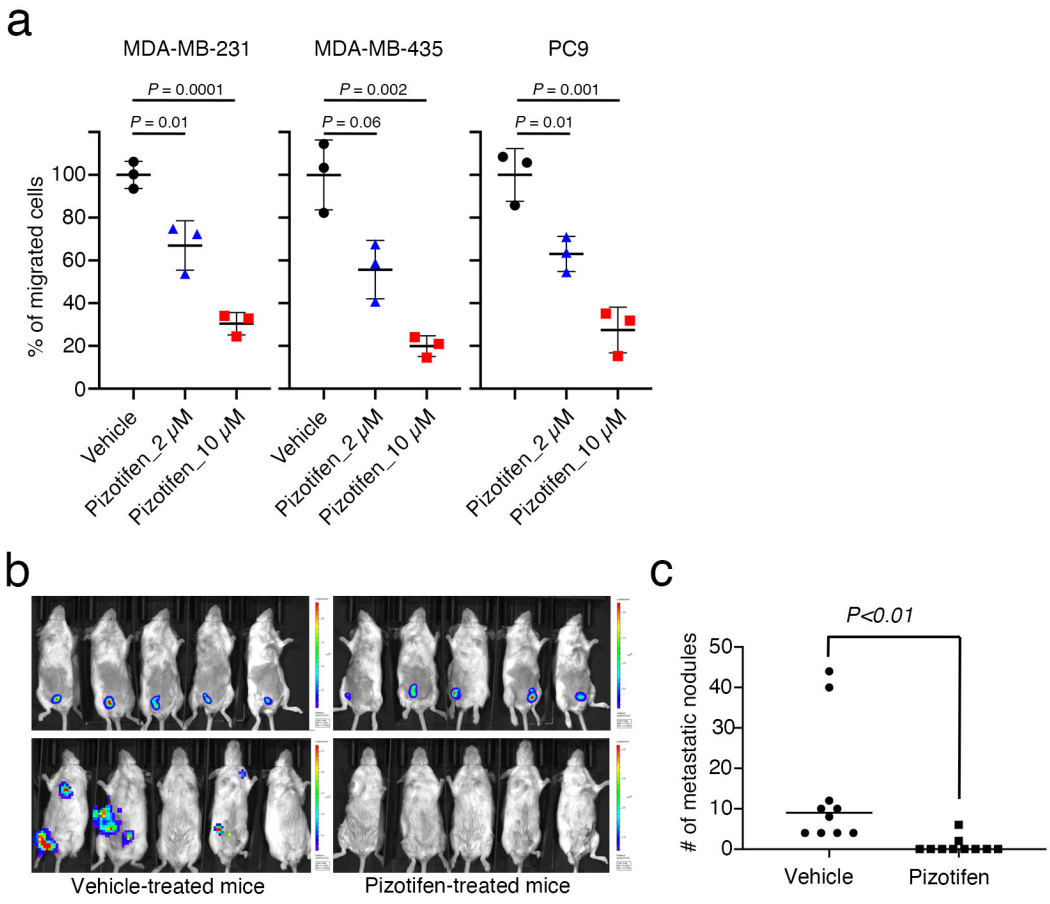

285

286 **Fig. 3_Pizotifen, one of epiboly-interrupting drugs, suppressed metastatic progression**

287 **of breast cancer cells in vitro and vivo**

288 **a**, Effect of pizotifen on cell motility and invasion of MBA-MB-231, MDA-MB-435, and

289 PC9 cells. Either vehicle or pizotifen treated the cells were subjected to Boyden chamber

290 assays. Fetal bovine serum (1% v/v) was used as the chemoattractant in both assays. Each

291 experiment was performed at least twice. **b**, Representative images of primary tumors on day

292 10 post-injection (top panels) and metastatic burden on day 70 post-injection (bottom panels)

293 taken using an IVIS Imaging System. **c**, Number of metastatic nodules in the lung of either

294 vehicle- or pizotifen-treated mice.

295

296 **Fig. 4**

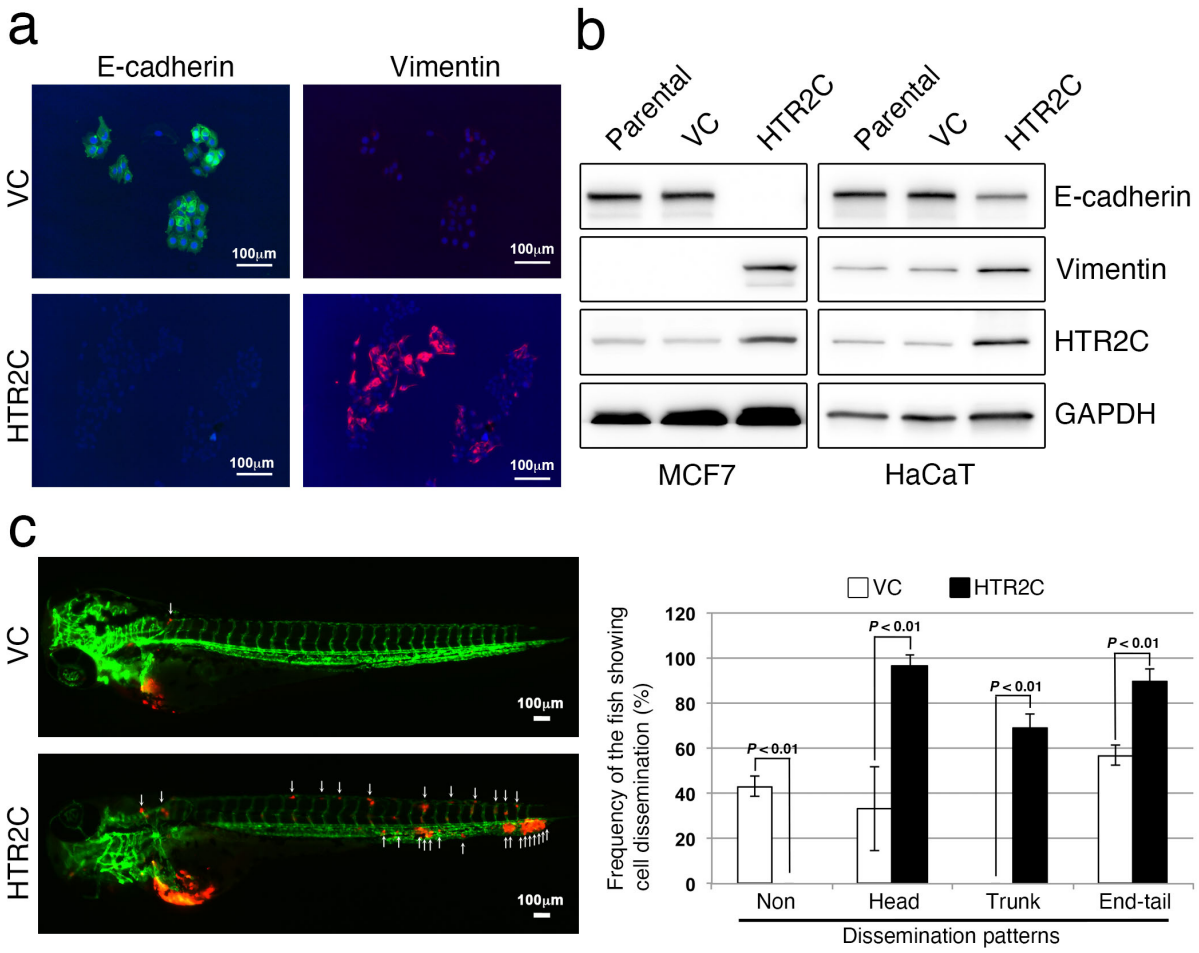

297

298 **Fig. 4_ HTR2C, a primary target of Pizotifen, induces epithelial-to-mesenchymal**

299 **transition (EMT)-mediated metastatic dissemination of human cancer cells**

300 **a**, Immunofluorescence staining of E-cadherin and vimentin expressions in the MCF7 cells.

301 **b**, Expression of E-cadherin and vimentin, and HTR2C were examined by western blotting in

302 the MCF7 and HaCaT cells; GAPDH loading control is shown (bottom). **c**, Representative

303 images of dissemination patterns of MCF7 cells expressing either the control vector (top left)

304 or HTR2C (lower left) in a zebrafish xenotransplantation model. White arrowheads indicate

305 disseminated MCF7 cells. The mean frequencies of the fish showing head, trunk, or end-tail

306 dissemination (right). Each value is indicated as the mean ± SEM of two independent

307 experiments. Statistical analysis was determined by Student's t test.

308 **Table 1. A list of the common fifty genes that are involved between gastrulation and**

309 **metastasis progression**

310

Genes	Gastrulation Defects	Ref	Effects in Metastasis	Ref
BMP	Convergence and extension	31	EMT	32
WNT	Convergence and extension	33	Migration and Invasion	34
FGF	Convergence and extension	35	Invision	36
EGF	Epiboly	37	Migration	38
PDGF	Convergence and extension	39	EMT	40
CXCL12	Migration of endodermal cells	41	Migration and Invasion	42
CXCR4	Migration of endodermal cells	41	Migration and Invasion	42
PIK3CA	Convergence and extension	43	Migration and Invasion	44
YES	Epiboly	45	Migration	46
FYN	Epiboly	47	Migration and Invasion	48
MAPK1	Epiboly	49	Migration	50
SHP2	Convergence and extension	51	Migration	52
SNAI1	Convergence and extension	53	EMT	54
SNAI2	Mesoderm & Neural crest formation	55	EMT	56
TWIST1	Mesoderm formation	57	EMT	58
TBXT	Convergence and extension	33	EMT	59
ZEB1	Epiboly	60	EMT	61
GSC	Mesodermal patterning	62	EMT	63
FOXC2	Unclear, defects in gastrulation	64	EMT	65
STAT3	Convergence and extension	66	Migration	67
POU5F1	Epiboly	68	EMT	69
EZH2	Unclear, defects in gastrulation	70	Invasion	71
EHMT2	Defects in Neurogenesis	72	Migration and Invasion	73
BMI1	Defects in skelton formation	74	EMT	75
RHOA	Convergence and extension	76	Migration and Invasion	77
CDC42	Convergence and extension	78	Migration and Invasion	79
RAC1	Convergence and extension	80	Migration and Invasion	81
ROCK2	Convergence and extension	82	Migration and Invasion	83
PAR1	Convergence and extension	84	Migration	85
PRKCI	Convergence and extension	84	EMT	86
CAP1	Convergence and extension	87	Migration	88
EZR	Epiboly	89	Migration	90
EPCAM	Epiboly	91	Migration and Invasion	92
ITGB1 / ITA5	Mesodermal Migration	93	Migration and Invasion	94
FN1	Convergence and extension	95	Invasion	96
HAS2	Dorsal migration of lateral cells	97	Invasion	98
MMP14	Convergence and extension	99	Invasion	100
COX1	Epiboly	101	Invasion	102
PTGES	Convergence and extension	103	Invasion	104
SLC39A6	Aterior migration	105	EMT	106
GNA12 / 13	Convergence and extension	72	Migration and Invasion	107
OGT	Epiboly	108	Migration and Invasion	109
CCN1	Cell Movement	110	Migration and Invasion	111
TRPM7	Convergence and extension	112	Migration	113
MAPKAPK2	Epiboly	114	Migration	115
B4GALT1	Convergence and extension	116	Invasion	117
IER2	Convergence and extension	118	Migration	119
TIP1	Convergence and extension	120	Migration and Invasion	121
PAK5	Convergence and extension	122	Migration	123
MARCKS	Convergence and extension	124	Migration and Invasion	125

311
312

313 References

314 1 MacRae, C. A. & Peterson, R. T. Zebrafish as tools for drug discovery. *Nature*
315 *REVIEWS* **14**, 721-731 (2015).
316 2 Zon, L. I. & Peterson, R. T. In vivo drug discovery in the zebrafish *Nat Rev Drug*
317 *Discov* **4**, 35-44 (2005).
318 3 Nakayama., J., Lu., J.-W., Makinoshima., H. & Gong., Z. A Novel Zebrafish Model of
319 Metastasis Identifies the HSD11β1 Inhibitor Adrenosterone as a Suppressor of
320 Epithelial-Mesenchymal Transition and Metastatic Dissemination. *Mol Cancer Res*
321 **18**, 477-487. (2020).
322 4 Nakayama, J. & Makinoshima, H. Zebrafish-Based Screening Models for the
323 Identification of Anti-Metastatic Drugs. *Molecules* **25**, 2407 (2020).
324 5 Nakayama, J. & Gong, Z. Transgenic zebrafish for modeling hepatocellular carcinoma.
325 *MedComm* **1**, 146-156. (2020).
326 6 Nguyen., D. X., Bos., P. D. & Massagué., J. Metastasis: from dissemination to organ-
327 specific colonization. *Nat Rev Cancer* **9**, 274-284 (2009).
328 7 Welch, D. R. & Hurst, D. R. Defining the Hallmarks of Metastasis *Cancer research* **79**,
329 3011-3027. (2019).
330 8 Chaffer, C. L. & Weinberg, R. A. A perspective on cancer cell metastasis *Science* **331**,
331 1559-1564 (2011).
332 9 Lu, W. & Kang, Y. Epithelial-Mesenchymal Plasticit in Cancer Progression and
333 Metastasis. *Developmental Cell* **49**, 361-374 (2019).
334 10 Tsai, J. H. & Yang, J. Epithelial–mesenchymal plasticity in carcinoma metastasis.
335 *Genes Dev* **27**, 2192-2206 (2013).
336 11 Solnica-Krezel, L. Conserved patterns of cell movements during vertebrate
337 gastrulation *Curr Biol* **15**, R213-228. , doi:10.1016/j.cub.2005.03.016. (2005).
338 12 White, R. J. *et al.* A high-resolution mRNA expression time course of embryonic
339 development in zebrafish. *eLife* **6** (2017).
340 13 Yang., J., Parker, A. & Geert, B. Guidelines and definitions for research on epithelial-
341 mesenchymal transition. *Nat Rev Mol Cell Biol* **21**, 341-352 (2020).
342 14 Nieto, M. A., Huang, R. Y.-J., Jackson, R. A. & Thiery, J. P. EMT: 2016 *Cell* **166**, 21-45
343 (2016).
344 15 Thiery, J. P., Acloque, H., Huang, R. Y. J. & Nieto, M. A. Epithelial-mesenchymal
345 transitions in development and disease *Cell* **139**, 871-890 (2009).
346 16 Yang, J. & Weinberg, R. A. Epithelial-mesenchymal transition: at the crossroads of
347 development and tumor metastasis *Dev Cell* **14**, 818-829 (2008).
348 17 Dongre, A. & Weinberg, R. A. New insights into the mechanisms of epithelial-
349 mesenchymal transition and implications for cancer. *Nat Rev Mol Cell Biol* 20, 69-84
350 (2019).
351 18 Nakayama, J. *et al.* HSD11β1 promotes EMT-mediated breast cancer metastasis.
352 *bioRxiv* **doi: https://doi.org/10.1101/2021.09.27.461934** (2021).
353 19 Nakayama, J. *et al.* A zebrafish embryo screen utilizing gastrulation identifies the
354 HTR2C inhibitor pizotifen as a suppressor of EMT-mediated metastasis. *Elife* ***10***,
355 e70151 (2021).
356 20 Nakayama, J., Konno, Y., Maruyama, A., Tomita, M. & Makinoshima, H. Cinnamon
357 bark extract suppresses metastatic dissemination of cancer cells through inhibition
358 of glycolytic metabolism *J Nat Med* (2022).

359 21 Gómez-Cuadrado, L., Tracey, N., Ma, R., Qian, B. & Brunton, V. G. Mouse models of
360 metastasis: progress and prospects *Dis Model Mech* **10**, 1061-1074. (2017).
361 22 Hoffman, R. M. Orthotopic metastatic (MetaMouse) models for discovery and
362 development of novel chemotherapy *Methods Mol Med* **111**, 297-322 (2005).
363 23 Chen, H.-C. Boyden chamber assay *Methods Mol Biol* **294**, 15-22 (2005).
364 24 Sack, U., Walther, W. & Scudiero, D. Novel effect of antihelminthic Niclosamide on
365 S100A4-mediated metastatic progression in colon cancer. *J Natl Cancer Inst* **103**,
366 1018-1036 (2011).
367 25 Itoh, K. *et al.* An essential part for Rho-associated kinase in the transcellular invasion
368 of tumor cells *Nat Med. 1999 Feb;5(2):* **2**, 221-225 (1999).
369 26 Marshall, J.-C. A. *et al.* Effect of inhibition of the lysophosphatidic acid receptor 1 on
370 metastasis and metastatic dormancy in breast cancer *J Natl Cancer Inst* **104**, 1306-
371 1319 (2012).
372 27 Gunnarsson, L., Jauhiainen, A., Kristiansson, E., Nerman, O. & Larsson, D. G. J.
373 Evolutionary conservation of human drug targets in organisms used for
374 environmental risk assessments. *Environmental Science & Technology* **42**, 5807–5813
375 (2008).
376 28 Pelka, K. E., Henn, K., Keck, A., Sapel, B. & Braunbeck, T. Size does matter –
377 Determination of the critical molecular size for the uptake of chemicals across the
378 chorion of zebrafish (Danio rerio) embryos. *Aquatic Toxicology* **185**, 1-10 (2017).
379 29 Urushibata, H. *et al.* Control of Developmental Speed in Zebrafish Embryos Using
380 Different Incubation Temperatures *Zebrafish* **18**, 316-325 (2021).
381 30 Yilmaz, O. *et al.* Scrambled eggs: Proteomic portraits and novel biomarkers of egg
382 quality in zebrafish (Danio rerio). *PLoS ONE* **12**, e0188084 (2017).
383 31 Kondo, M. Bone morphogenetic proteins in the early development of zebrafish. *FEBS*
384 *J* **274**, 2960-2967, doi:10.1111/j.1742-4658.2007.05838.x (2007).
385 32 Katsuno, Y. *et al.* Bone morphogenetic protein signaling enhances invasion and bone
386 metastasis of breast cancer cells through Smad pathway. *Oncogene* **27**, 6322-6333,
387 doi:10.1038/onc.2008.232 (2008).
388 33 Tada, M. & Smith, J. C. Xwnt11 is a target of Xenopus Brachyury: regulation of
389 gastrulation movements via Dishevelled, but not through the canonical Wnt
390 pathway. *Development* **127**, 2227-2238 (2000).
391 34 Vincan, E. & Barker, N. The upstream components of the Wnt signalling pathway in
392 the dynamic EMT and MET associated with colorectal cancer progression. *Clin Exp*
393 *Metastasis* **25**, 657-663, doi:10.1007/s10585-008-9156-4 (2008).
394 35 Yang, X., Dormann, D., Munsterberg, A. E. & Weijer, C. J. Cell movement patterns
395 during gastrulation in the chick are controlled by positive and negative chemotaxis
396 mediated by FGF4 and FGF8. *Dev Cell* **3**, 425-437 (2002).
397 36 Nomura, S. *et al.* FGF10/FGFR2 signal induces cell migration and invasion in
398 pancreatic cancer. *Br J Cancer* **99**, 305-313, doi:10.1038/sj.bjc.6604473 (2008).
399 37 Song, S. *et al.* Pou5f1-dependent EGF expression controls E-cadherin endocytosis,
400 cell adhesion, and zebrafish epiboly movements. *Dev Cell* **24**, 486-501,
401 doi:10.1016/j.devcel.2013.01.016 (2013).
402 38 Lu, Z., Jiang, G., Blume-Jensen, P. & Hunter, T. Epidermal growth factor-induced
403 tumor cell invasion and metastasis initiated by dephosphorylation and
404 downregulation of focal adhesion kinase. *Mol Cell Biol* **21**, 4016-4031,
405 doi:10.1128/MCB.21.12.4016-4031.2001 (2001).

406 39 Damm, E. W. & Winklbauer, R. PDGF-A controls mesoderm cell orientation and radial
407 intercalation during Xenopus gastrulation. *Development* **138**, 565-575,
408 doi:10.1242/dev.056903 (2011).
409 40 Jechlinger, M. *et al.* Autocrine PDGFR signaling promotes mammary cancer
410 metastasis. *J Clin Invest* **116**, 1561-1570, doi:10.1172/JCI24652 (2006).
411 41 Mizoguchi, T., Verkade, H., Heath, J. K., Kuroiwa, A. & Kikuchi, Y. Sdf1/Cxcr4 signaling
412 controls the dorsal migration of endodermal cells during zebrafish gastrulation.
413 *Development* **135**, 2521-2529, doi:10.1242/dev.020107 (2008).
414 42 Shen, H. B., Gu, Z. Q., Jian, K. & Qi, J. CXCR4-mediated Stat3 activation is essential for
415 CXCL12-induced cell invasion in bladder cancer. *Tumour Biol* **34**, 1839-1845,
416 doi:10.1007/s13277-013-0725-z (2013).
417 43 Montero, J.-A., Kilian, B., Chan, J., Bayliss, P. E. & Heisenberg, C.-P. Phosphoinositide
418 3-Kinase Is Required for Process Outgrowth and Cell Polarization of Gastrulating
419 Mesendodermal Cells. *Current Biology* **13**, 1279-1289, doi:10.1016/s0960-
420 9822(03)00505-0 (2003).
421 44 Wander, S. A. *et al.* PI3K/mTOR inhibition can impair tumor invasion and metastasis
422 in vivo despite a lack of antiproliferative action in vitro: implications for targeted
423 therapy. *Breast Cancer Res Treat* **138**, 369-381, doi:10.1007/s10549-012-2389-6
424 (2013).
425 45 Tsai, W. B., Zhang, X., Sharma, D., Wu, W. & Kinsey, W. H. Role of Yes kinase during
426 early zebrafish development. *Dev Biol* **277**, 129-141,
427 doi:10.1016/j.ydbio.2004.08.052 (2005).
428 46 Barraclough, J., Hodgkinson, C., Hogg, A., Dive, C. & Welman, A. Increases in c-Yes
429 Expression Level and Activity Promote Motility But Not Proliferation of Human
430 Colorectal Carcinoma Cells. *Neoplasia* **9**, 745-IN732, doi:10.1593/neo.07442 (2007).
431 47 Sharma, D., Holets, L., Zhang, X. & Kinsey, W. H. Role of Fyn kinase in signaling
432 associated with epiboly during zebrafish development. *Dev Biol* **285**, 462-476,
433 doi:10.1016/j.ydbio.2005.07.018 (2005).
434 48 Yadav, V. & Denning, M. F. Fyn is induced by Ras/PI3K/Akt signaling and is required
435 for enhanced invasion/migration. *Mol Carcinog* **50**, 346-352, doi:10.1002/mc.20716
436 (2011).
437 49 Krens, S. F. *et al.* Distinct functions for ERK1 and ERK2 in cell migration processes
438 during zebrafish gastrulation. *Dev Biol* **319**, 370-383,
439 doi:10.1016/j.ydbio.2008.04.032 (2008).
440 50 Radtke, S., Milanovic, M. & Rossé, C. ERK2 but not ERK1 mediates HGF-induced
441 motility in non-small cell lung carcinoma cell lines. *J Cell Sci.* **126**, 2381-2391 (2013).
442 51 Jopling, C., van Geemen, D. & den Hertog, J. Shp2 knockdown and Noonan/LEOPARD
443 mutant Shp2-induced gastrulation defects. *PLoS Genet* **3**, e225,
444 doi:10.1371/journal.pgen.0030225 (2007).
445 52 Wang, F. M. *et al.* SHP-2 promoting migration and metastasis of MCF-7 with loss of
446 E-cadherin, dephosphorylation of FAK and secretion of MMP-9 induced by IL-1beta
447 in vivo and in vitro. *Breast Cancer Res Treat* **89**, 5-14, doi:10.1007/s10549-004-1002-
448 z (2005).
449 53 Ip, Y. T. & Gridley, T. Cell movements during gastrulation: snail dependent and
450 independent pathways. *Curr Opin Genet Dev* **12**, 423-429 (2002).

451 54 Batlle, E., Sancho, E., Francí, C., Domínguez, D. & Monfar, M. The transcription factor
452 snail is a repressor of E-cadherin gene expression in epithelial tumour cells. *Nat Cell*
453 *Biol* **2**, 84-89 (2000).
454 55 Shi, J., Severson, C., Yang, J., Wedlich, D. & Klymkowsky, M. W. Snail2 controls
455 mesodermal BMP/Wnt induction of neural crest. *Development* **138**, 3135-3145,
456 doi:10.1242/dev.064394 (2011).
457 56 Medici, D., Hay, E. D. & B.R., O. Snail and Slug Promote Epithelial-Mesenchymal
458 Transition through -Catenin–T-Cell Factor-4-dependent Expression of Transforming
459 Growth Factor-3. *Molecular Biology of the Cell* **19**, 4875–4887, doi:10.1091/mbc.E08
460 (2008).
461 57 Castanon, I. & Baylies, M. K. A Twist in fate: evolutionary comparison of Twist
462 structure and function. *Gene* **287**, 11-22 (2002).
463 58 Yang, J. *et al.* Twist, a master regulator of morphogenesis, plays an essential role in
464 tumor metastasis. *Cell* **117**, 927-939, doi:10.1016/j.cell.2004.06.006 (2004).
465 59 Fernando, R. I. *et al.* The T-box transcription factor Brachyury promotes epithelial-
466 mesenchymal transition in human tumor cells. *J Clin Invest* **120**, 533-544,
467 doi:10.1172/JCI38379 (2010).
468 60 Vannier, C., Mock, K., Brabletz, T. & Driever, W. Zeb1 regulates E-cadherin and
469 Epcam (epithelial cell adhesion molecule) expression to control cell behavior in early
470 zebrafish development. *J Biol Chem* **288**, 18643-18659,
471 doi:10.1074/jbc.M113.467787 (2013).
472 61 Spaderna, S. *et al.* The transcriptional repressor ZEB1 promotes metastasis and loss
473 of cell polarity in cancer. *Cancer Res* **68**, 537-544, doi:10.1158/0008-5472.CAN-07-
474 5682 (2008).
475 62 Sander, V., Reversade, B. & De Robertis, E. M. The opposing homeobox genes
476 Goosecoid and Vent1/2 self-regulate Xenopus patterning. *EMBO J* **26**, 2955-2965,
477 doi:10.1038/sj.emboj.7601705 (2007).
478 63 Hartwell, K. A. *et al.* The Spemann organizer gene, Goosecoid, promotes tumor
479 metastasis. *Proc Natl Acad Sci U S A* **103**, 18969-18974,
480 doi:10.1073/pnas.0608636103 (2006).
481 64 Wilm, B., James, R. G., Schultheiss, T. M. & Hogan, B. L. The forkhead genes, Foxc1
482 and Foxc2, regulate paraxial versus intermediate mesoderm cell fate. *Dev Biol* **271**,
483 176-189, doi:10.1016/j.ydbio.2004.03.034 (2004).
484 65 Mani, S. A. *et al.* Mesenchyme Forkhead 1 (FOXC2) plays a key role in metastasis and
485 is associated with aggressive basal-like breast cancers. *Proc Natl Acad Sci U S A* **104**,
486 10069-10074, doi:10.1073/pnas.0703900104 (2007).
487 66 Miyagi, C. *et al.* STAT3 noncell-autonomously controls planar cell polarity during
488 zebrafish convergence and extension. *J Cell Biol* **166**, 975-981,
489 doi:10.1083/jcb.200403110 (2004).
490 67 Abdulghani, J. *et al.* Stat3 promotes metastatic progression of prostate cancer. *Am J*
491 *Pathol* **172**, 1717-1728, doi:10.2353/ajpath.2008.071054 (2008).
492 68 Lachnit, M., Kur, E. & Driever, W. Alterations of the cytoskeleton in all three
493 embryonic lineages contribute to the epiboly defect of Pou5f1/Oct4 deficient MZspg
494 zebrafish embryos. *Dev Biol* **315**, 1-17, doi:10.1016/j.ydbio.2007.10.008 (2008).
495 69 Dai, X. *et al.* OCT4 regulates epithelial-mesenchymal transition and its knockdown
496 inhibits colorectal cancer cell migration and invasion. *Oncol Rep* **29**, 155-160,
497 doi:10.3892/or.2012.2086 (2013).

498 70 O'Carroll, D. *et al.* The polycomb-group gene Ezh2 is required for early mouse
499 development. *Mol Cell Biol* **21**, 4330-4336, doi:10.1128/MCB.21.13.4330-4336.2001
500 (2001).
501 71 Ren, G. *et al.* Polycomb protein EZH2 regulates tumor invasion via the transcriptional
502 repression of the metastasis suppressor RKIP in breast and prostate cancer. *Cancer*
503 *Res* **72**, 3091-3104, doi:10.1158/0008-5472.CAN-11-3546 (2012).
504 72 Lin, F. *et al.* Essential roles of G{alpha}12/13 signaling in distinct cell behaviors
505 driving zebrafish convergence and extension gastrulation movements. *J Cell Biol* **169**,
506 777-787, doi:10.1083/jcb.200501104 (2005).
507 73 Chen, M. W. *et al.* H3K9 histone methyltransferase G9a promotes lung cancer
508 invasion and metastasis by silencing the cell adhesion molecule Ep-CAM. *Cancer Res*
509 **70**, 7830-7840, doi:10.1158/0008-5472.CAN-10-0833 (2010).
510 74 van der Lugt, N. M. *et al.* Posterior transformation, neurological abnormalities, and
511 severe hematopoietic defects in mice with a targeted deletion of the bmi-1 proto-
512 oncogene. *Genes Dev* **8**, 757-769 (1994).
513 75 Guo, B. H. *et al.* Bmi-1 promotes invasion and metastasis, and its elevated expression
514 is correlated with an advanced stage of breast cancer. *Mol Cancer* **10**, 10,
515 doi:10.1186/1476-4598-10-10 (2011).
516 76 Zhu, S., Liu, L., Korzh, V., Gong, Z. & Low, B. C. RhoA acts downstream of Wnt5 and
517 Wnt11 to regulate convergence and extension movements by involving effectors
518 Rho kinase and Diaphanous: use of zebrafish as an in vivo model for GTPase
519 signaling. *Cell Signal* **18**, 359-372, doi:10.1016/j.cellsig.2005.05.019 (2006).
520 77 Yoshioka, K., Nakamori, S. & Itoh, K. Overexpression of small GTP-binding protein
521 RhoA promotes invasion of tumor cells. *Cancer Res* **59**, 2004-2010 (1999).
522 78 Choi, S. C. & Han, J. K. Xenopus Cdc42 regulates convergent extension movements
523 during gastrulation through Wnt/Ca2+ signaling pathway. *Dev Biol* **244**, 342-357,
524 doi:10.1006/dbio.2002.0602 (2002).
525 79 Reymond, N. *et al.* Cdc42 promotes transendothelial migration of cancer cells
526 through beta1 integrin. *J Cell Biol* **199**, 653-668, doi:10.1083/jcb.201205169 (2012).
527 80 Habas, R., Dawid, I. B. & He, X. Coactivation of Rac and Rho by Wnt/Frizzled signaling
528 is required for vertebrate gastrulation. . *Genes Dev* **17**, 295-309., doi:10.1101/
529 (2003).
530 81 Vega, F. M. & Ridley, A. J. Rho GTPases in cancer cell biology. *FEBS Lett* **582**, 2093-
531 2101, doi:10.1016/j.febslet.2008.04.039 (2008).
532 82 Marlow, F., Topczewski, J., Sepich, D. & Solnica-Krezel, L. Zebrafish Rho kinase 2 acts
533 downstream of Wnt11 to mediate cell polarity and effective convergence and
534 extension movements. *Curr Biol* **12**, 876-884 (2002).
535 83 Itoh, K. *et al.* An essential part for Rho-associated kinase in the transcellular invasion
536 of tumor cells. *Nat Med* **5**, 221-225, doi:10.1038/5587 (1999).
537 84 Kusakabe, M. & Nishida, E. The polarity-inducing kinase Par-1 controls Xenopus
538 gastrulation in cooperation with 14-3-3 and aPKC. *EMBO J* **23**, 4190-4201,
539 doi:10.1038/sj.emboj.7600381 (2004).
540 85 Shi, X., Gangadharan, B., Brass, L. F., Ruf, W. & Mueller, B. M. Protease-activated
541 receptors (PAR1 and PAR2) contribute to tumor cell motility and metastasis. *Mol*
542 *Cancer Res* **2**, 395-402 (2004).
543 86 Gunaratne, A., Thai, B. L. & Di Guglielmo, G. M. Atypical protein kinase C
544 phosphorylates Par6 and facilitates transforming growth factor beta-induced

545 epithelial-to-mesenchymal transition. *Mol Cell Biol* **33**, 874-886,
546 doi:10.1128/MCB.00837-12 (2013).
547 87 Seifert, K., Ibrahim, H., Stodtmeister, T., Winklbauer, R. & Niessen, C. M. An
548 adhesion-independent, aPKC-dependent function for cadherins in morphogenetic
549 movements. *J Cell Sci* **122**, 2514-2523, doi:10.1242/jcs.042796 (2009).
550 88 Yamazaki, K. *et al.* Adenylate cyclase-associated protein 1 overexpressed in
551 pancreatic cancers is involved in cancer cell motility. *Lab Invest* **89**, 425-432,
552 doi:10.1038/labinvest.2009.5 (2009).
553 89 Link, V. *et al.* Identification of regulators of germ layer morphogenesis using
554 proteomics in zebrafish. *J Cell Sci* **119**, 2073-2083, doi:10.1242/jcs.02928 (2006).
555 90 Khanna, C. *et al.* The membrane-cytoskeleton linker ezrin is necessary for
556 osteosarcoma metastasis. *Nat Med* **10**, 182-186, doi:10.1038/nm982 (2004).
557 91 Slanchev, K. *et al.* The epithelial cell adhesion molecule EpCAM is required for
558 epithelial morphogenesis and integrity during zebrafish epiboly and skin
559 development. *PLoS Genet* **5**, e1000563, doi:10.1371/journal.pgen.1000563 (2009).
560 92 Ni, J. *et al.* Role of the EpCAM (CD326) in prostate cancer metastasis and
561 progression. *Cancer Metastasis Rev* **31**, 779-791, doi:10.1007/s10555-012-9389-1
562 (2012).
563 93 Skalski, M., Alfandari, D. & Darribere, T. A key function for alphav containing
564 integrins in mesodermal cell migration during Pleurodeles waltl gastrulation. *Dev Biol*
565 **195**, 158-173, doi:10.1006/dbio.1997.8838 (1998).
566 94 Felding-Habermann, B. Integrin adhesion receptors in tumor metastasis. *Clin Exp*
567 *Metastasis* **20**, 203-213 (2003).
568 95 Marsden, M. & DeSimone, D. W. Integrin-ECM Interactions Regulate Cadherin-
569 Dependent Cell Adhesion and Are Required for Convergent Extension in Xenopus.
570 *Current Biology* **13**, 1182-1191, doi:10.1016/s0960-9822(03)00433-0 (2003).
571 96 Malik, G. *et al.* Plasma fibronectin promotes lung metastasis by contributions to
572 fibrin clots and tumor cell invasion. *Cancer Res* **70**, 4327-4334, doi:10.1158/0008-
573 5472.CAN-09-3312 (2010).
574 97 Bakkers, J. *et al.* Has2 is required upstream of Rac1 to govern dorsal migration of
575 lateral cells during zebrafish gastrulation. *Development* **131**, 525-537,
576 doi:10.1242/dev.00954 (2004).
577 98 Kim, H. R. *et al.* Hyaluronan facilitates invasion of colon carcinoma cells in vitro via
578 interaction with CD44. *Cancer Res* **64**, 4569-4576, doi:10.1158/0008-5472.CAN-04-
579 0202 (2004).
580 99 Coyle, R. C., Latimer, A. & Jessen, J. R. Membrane-type 1 matrix metalloproteinase
581 regulates cell migration during zebrafish gastrulation: evidence for an interaction
582 with non-canonical Wnt signaling. *Exp Cell Res* **314**, 2150-2162,
583 doi:10.1016/j.yexcr.2008.03.010 (2008).
584 100 Perentes, J. Y. *et al.* Cancer cell-associated MT1-MMP promotes blood vessel
585 invasion and distant metastasis in triple-negative mammary tumors. *Cancer Res* **71**,
586 4527-4538, doi:10.1158/0008-5472.CAN-10-4376 (2011).
587 101 Cha, Y. I. *et al.* Cyclooxygenase-1-derived PGE2 promotes cell motility via the G-
588 protein-coupled EP4 receptor during vertebrate gastrulation. *Genes Dev* **20**, 77-86,
589 doi:10.1101/gad.1374506 (2006).

590 102 Kundu, N. & Fulton, A. M. Selective cyclooxygenase (COX)-1 or COX-2 inhibitors
591 control metastatic disease in a murine model of breast cancer. *Cancer Res* **62**, 2343-
592 2346 (2002).
593 103 Speirs, C. K. *et al.* Prostaglandin Gbetagamma signaling stimulates gastrulation
594 movements by limiting cell adhesion through Snai1a stabilization. *Development* **137**,
595 1327-1337, doi:10.1242/dev.045971 (2010).
596 104 Wang, D. & Dubois, R. N. Prostaglandins and cancer. *Gut* **55**, 115-122,
597 doi:10.1136/gut.2004.047100 (2006).
598 105 Yamashita, S. *et al.* Zinc transporter LIVI controls epithelial-mesenchymal transition
599 in zebrafish gastrula organizer. *Nature* **429**, 298-302, doi:10.1038/nature02545
600 (2004).
601 106 Lue, H. W. *et al.* LIV-1 promotes prostate cancer epithelial-to-mesenchymal
602 transition and metastasis through HB-EGF shedding and EGFR-mediated ERK
603 signaling. *PLoS One* **6**, e27720, doi:10.1371/journal.pone.0027720 (2011).
604 107 Yagi, H. *et al.* A synthetic biology approach reveals a CXCR4-G13-Rho signaling axis
605 driving transendothelial migration of metastatic breast cancer cells. *Sci Signal* **4**,
606 ra60, doi:10.1126/scisignal.2002221 (2011).
607 108 Webster, D. M. *et al.* O-GlcNAc modifications regulate cell survival and epiboly
608 during zebrafish development. *BMC Dev Biol* **9**, 28, doi:10.1186/1471-213X-9-28
609 (2009).
610 109 Lynch, T. P. *et al.* Critical role of O-Linked beta-N-acetylglucosamine transferase in
611 prostate cancer invasion, angiogenesis, and metastasis. *J Biol Chem* **287**, 11070-
612 11081, doi:10.1074/jbc.M111.302547 (2012).
613 110 Latinkic, B. V. Xenopus Cyr61 regulates gastrulation movements and modulates Wnt
614 signalling. *Development* **130**, 2429-2441, doi:10.1242/dev.00449 (2003).
615 111 Lin, J. *et al.* A novel anti-Cyr61 antibody inhibits breast cancer growth and metastasis
616 in vivo. *Cancer Immunol Immunother* **61**, 677-687, doi:10.1007/s00262-011-1135-y
617 (2012).
618 112 Liu, W. *et al.* TRPM7 regulates gastrulation during vertebrate embryogenesis. *Dev*
619 *Biol* **350**, 348-357, doi:10.1016/j.ydbio.2010.11.034 (2011).
620 113 Middelbeek, J. *et al.* TRPM7 is required for breast tumor cell metastasis. *Cancer Res*
621 **72**, 4250-4261, doi:10.1158/0008-5472.CAN-11-3863 (2012).
622 114 Holloway, B. A. *et al.* A novel role for MAPKAPK2 in morphogenesis during zebrafish
623 development. *PLoS Genet* **5**, e1000413, doi:10.1371/journal.pgen.1000413 (2009).
624 115 Kumar, B. *et al.* p38 mitogen-activated protein kinase-driven MAPKAPK2 regulates
625 invasion of bladder cancer by modulation of MMP-2 and MMP-9 activity. *Cancer Res*
626 **70**, 832-841, doi:10.1158/0008-5472.CAN-09-2918 (2010).
627 116 Machingo, Q. J., Fritz, A. & Shur, B. D. A beta1,4-galactosyltransferase is required for
628 convergent extension movements in zebrafish. *Dev Biol* **297**, 471-482,
629 doi:10.1016/j.ydbio.2006.05.024 (2006).
630 117 Zhu, X. *et al.* Elevated beta1,4-galactosyltransferase I in highly metastatic human
631 lung cancer cells. Identification of E1AF as important transcription activator. *J Biol*
632 *Chem* **280**, 12503-12516, doi:10.1074/jbc.M413631200 (2005).
633 118 Hong, S. K., Tanegashima, K. & Dawid, I. B. XIer2 is required for convergent extension
634 movements during Xenopus development. *Int J Dev Biol* **55**, 917-921,
635 doi:10.1387/ijdb.113288sh (2011).

636 119 Neeb, A. *et al.* The immediate early gene Ier2 promotes tumor cell motility and
637 metastasis, and predicts poor survival of colorectal cancer patients. *Oncogene* **31**,
638 3796-3806, doi:10.1038/onc.2011.535 (2012).
639 120 Besser, J., Leito, J. T., van der Meer, D. L. & Bagowski, C. P. Tip-1 induces filopodia
640 growth and is important for gastrulation movements during zebrafish development.
641 *Dev Growth Differ* **49**, 205-214, doi:10.1111/j.1440-169X.2007.00921.x (2007).
642 121 Han, M., Wang, H., Zhang, H. T. & Han, Z. The PDZ protein TIP-1 facilitates cell
643 migration and pulmonary metastasis of human invasive breast cancer cells in
644 athymic mice. *Biochem Biophys Res Commun* **422**, 139-145,
645 doi:10.1016/j.bbrc.2012.04.123 (2012).
646 122 Faure, S. *et al.* Xenopus p21-activated kinase 5 regulates blastomeres' adhesive
647 properties during convergent extension movements. *Dev Biol* **277**, 472-492,
648 doi:10.1016/j.ydbio.2004.10.005 (2005).
649 123 Gong, W. *et al.* P21-activated kinase 5 is overexpressed during colorectal cancer
650 progression and regulates colorectal carcinoma cell adhesion and migration. *Int J*
651 *Cancer* **125**, 548-555, doi:10.1002/ijc.24428 (2009).
652 124 Iioka, H., Ueno, N. & Kinoshita, N. Essential role of MARCKS in cortical actin dynamics
653 during gastrulation movements. *J Cell Biol* **164**, 169-174, doi:10.1083/jcb.200310027
654 (2004).
655 125 Rombouts, K. *et al.* Myristoylated Alanine-Rich protein Kinase C Substrate (MARCKS)
656 expression modulates the metastatic phenotype in human and murine colon
657 carcinoma in vitro and in vivo. *Cancer Lett* **333**, 244-252,
658 doi:10.1016/j.canlet.2013.01.040 (2013).
659